Nonlinear Models for the Intermodulation Analysis of FET Mixers

Solti Peng, *Student Member, IEEE,* Patrick J. McCleer, *Member, IEEE,* and George I. Haddad, *Fellow, IEEE*

***Abstract*—An accurate, detailed analysis program has been developed for intermodulation distortion (IMD) simulation of FET mixers. This program is very efficient at calculating the IMD from multiple RF inputs. We have proposed a simplified nonlinear model for IMD analysis of FET gate mixers. The accuracy of the simplified model has been verified experimentally using two different MESFET mixers and one HEMT mixer at X band. All the tests show good agreement between measured results and the calculated results for second- and third-order IMD. The simplified model is based on modeling the derivative of the device transconductance by a sum of a Gaussian function and a linear function of the gate voltage. Drain bias dependence is ignored. The advantage of this model is that it can be used for both MESFET and HEMT mixers, and its fitting parameters can be easily determined from a nonlinear characterization of the devices at low frequencies.**

I. Introduction

THE demand for a wide dynamic range in today's microwave and millimeter-wave receivers results in strict IMD performance requirements for the front-end mixers. MESFET mixers, due to their low intermodulation products and low noise, as well as the potential for conversion gain, are gaining favor over their counterparts, diode mixers, because they can be easily realized in MMIC's. In order to effectively describe the IMD performance of the FET mixers, an efficient and accurate analysis tool is required. In recent years, the harmonic balance technique [1]–[4] and Volterra series [5], [6] expansion have been widely used in the microwave nonlinear circuit simulations. Also, the general-purpose harmonic balance technique has been broadly implemented in commercial microwave nonlinear circuit simulators. Nonetheless, the IMD of FET mixers is still rarely included in the circuit simulation during the mixer design. The reasons are, since there are one large LO signal and two RF small signals occurring in the IMD analysis in mixers, the efficiency of the harmonic balance technique dramatically drops with the number of input signals, and the IMD from small signals under the presence of a large signal will be smeared out due to the numerical accuracy of computers. The Volterra series is very efficient at analyzing multiple inputs, but it is limited to moderate power inputs and not suitable for the large signal input encountered in the mixer IMD analysis. The only way to avoid these problems is to analyze the large signal and small signals separately, using the harmonic balance technique for large-signal analysis and Volterra series for small-signal analysis. We have applied this technique to FET mixers. Our work is based on the pioneering work of Maas [7] who used this technique to calculate the two-tone IMD in diode mixers.

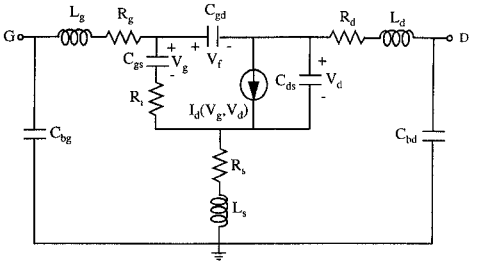

Fig. 1. FET large-signal equivalent circuit. Bonding parasitics are included.

An accurate device circuit model is required for IMD analysis. This model must both include the nonlinear elements and account for the derivatives of functional dependence of these nonlinear elements at least up to third order [8], [9]. Most of the existing nonlinear models for FET's, however, are not in this category [10]–[13]. Two models [8], [14] consider the derivative terms, but do not include a good description of the third-order derivative. Also, the fitting of the derivatives of their models to the measured data is not intuitive. Therefore, a simple FET nonlinear model suitable for mixer IM analysis is sought.

A brief description of the analysis program is given in the next section. We apply this analysis program to study the nonlinear drain current source contribution to the overall IMD performance of MESFET mixers at X band. Then, we propose a nonlinear model which simplifies the derivatives fitting process, and also gives good agreement between the measured and fitted nonlinear element value and its derivatives. We then present experimental and calculated results of the IMD performance in two MESFET mixers and one HEMT mixer at X band.

II. The Analysis Program

An efficient and accurate analysis program has been developed for IMD simulation of FET mixers. The technique used in this program is based on the *large-signal–small-signal*

Manuscript received April 5, 1994; revised July 18, 1994. This work was supported by the U.S. Army Research Office under the URI Program Grant DAAL03-92-G-0109.

The authors are with the Center for High Frequency Microelectronics, Solid State Electronics Laboratory, Department of Electrical Engineering and Computer Science, University of Michigan, Ann Arbor, MI 48109 USA.

IEEE Log Number 9410324.

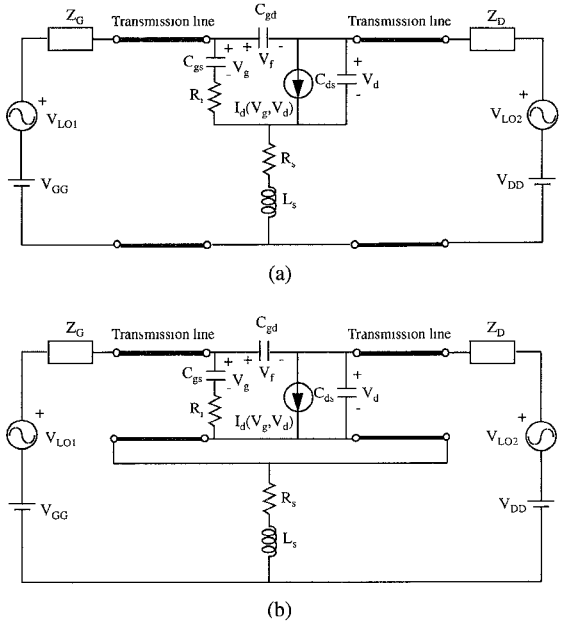

Fig. 2. (a) An intuitive FET circuit layout and (b) a modified FET circuit layout for large-signal harmonic balance analysis using the reflection algorithm.

analysis [15]. The equivalent circuit of the device used in the large signal analysis is shown in Fig. 1. The reflection algorithm [16], [17] is used for the large-signal harmonic-balance analysis to obtain the LO pumping waveforms for the voltages across the internal capacitors. This algorithm is constructed by using two ideal imaginary transmission lines, with their electrical lengths at the LO frequency equal to many half wavelengths to isolate the nonlinear device from the linear input and output circuits. The steady-state solution of the device is solved in the time domain. The voltage and current waveforms at the other end of the imaginary transmission lines are expanded into Fourier series at the LO harmonic components. In order to pursue the match of the impedance of the Fourier components to the impedance of the linear circuit at the LO harmonic frequencies, iterations are carried out by summing up the reflected waves due to the impedance mismatch until they are matched. An intuitive circuit topology [18] of this case is shown in Fig. 2(a). A drawback of this intuitive case is that the time-domain equation of the device is rather complicated. Theoretically, the imaginary transmission lines can be placed at any position in the circuit without altering the steady-state solution of the circuit. Therefore, we should keep the part of the time-domain equations as simple as possible. The best choice is to include only nonlinear elements and to move all linear elements to the other side of the imaginary transmission lines. The advantages are: saving computer running time, avoiding the possible numerical convergence problem, and the ease with which to include possible linear reactive elements without modifying the part of the time-domain equations. The new circuit topology for the large-signal analysis is shown in Fig. 2(b) which excludes the source impedance (series source resistance and source bonding inductance) from

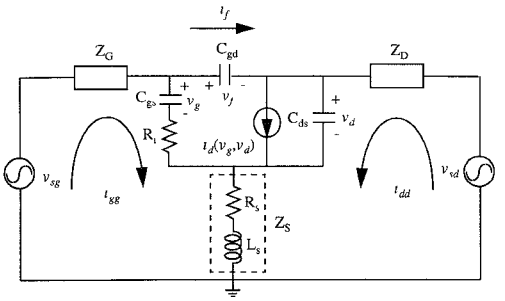

Fig. 3. The equivalent circuit for small-signal analysis.

the nonlinear part of the circuit. The capacitors C_{gd} and C_{ds}, which can be treated as linear elements in the FET gate mixers, are still included in the nonlinear part of the circuit in order to increase the flexibility of the program, i.e., to include their nonlinearities, if needed. The internal voltage waveforms of V_g, V_f, and V_d are obtained by the reflection algorithm according to the new circuit topology.

The FET small-signal equivalent circuit is shown in Fig. 3. The small-signal incremental current loop equations can be written in the following matrix form:

$$\boldsymbol{ZI} = \boldsymbol{V} \tag{1}$$

where

$$\boldsymbol{Z} = \begin{pmatrix} Z_G + R_i + Z_S & Z_G & Z_S \\ Z_G & Z_G + Z_D & -Z_D \\ Z_S & -Z_D & Z_D + Z_S \end{pmatrix} \tag{2}$$

$$\boldsymbol{I} = \begin{pmatrix} i_{gg}(t) \\ i_f(t) \\ i_{dd}(t) \end{pmatrix} \tag{3}$$

$$\boldsymbol{V} = \begin{pmatrix} v_{sg}(t) - v_g(t) \\ v_{sg}(t) - v_{sd}(t) - v_f(t) \\ v_{sd}(t) - v_d(t) \end{pmatrix} \tag{4}$$

where i_{gg}, i_f, i_{dd} are small-signal incremental currents, v_g, v_f, v_d are small-signal incremental voltages, and v_{sg}, v_{sd} are small-signal voltage sources at gate and drain, respectively.

Since the most significant nonlinear element in a MESFET gate mixer is the drain current, the nonlinear effects from the capacitors are ignored in our work. Thus, the small-signal incremental currents are

$$i_{gg} = \frac{d}{dt}(C_{gs} v_g(t)) \tag{5}$$

$$i_f = \frac{d}{dt}(C_{gd} v_f(t)) \tag{6}$$

$$i_{dd} = i_d(v_g, v_d) + \frac{d}{dt}(C_{ds} v_d(t)). \tag{7}$$

The small-signal drain current $i_d(v_g, v_d)$, expanded in Taylor's series up to third order, is as follows:

$$\begin{aligned} i_d(v_g, v_d) &= \frac{\partial I_d}{\partial V_g} v_g + \frac{\partial I_d}{\partial V_d} v_d + \frac{1}{2}\frac{\partial^2 I_d}{\partial V_g^2} v_g^2 \\ &\quad + \frac{\partial^2 I_d}{\partial V_g \partial V_d} v_g v_d + \frac{1}{2}\frac{\partial^2 I_d}{\partial V_d^2} v_d^2 \\ &\quad + \frac{1}{6}\frac{\partial^3 I_d}{\partial V_g^3} v_g^3 + \frac{1}{2}\frac{\partial^3 I_d}{\partial V_g^2 \partial V_d} v_g^2 v_d \\ &\quad + \frac{1}{2}\frac{\partial^3 I_d}{\partial V_g \partial V_d^2} v_g v_d^2 + \frac{1}{6}\frac{\partial^3 I_d}{\partial V_d^3} v_d^3 \\ &\equiv G_m v_g \\ &\quad + G_{ds} v_d + G_{m2} v_g^2 \\ &\quad + G_{m1d1} v_g v_d + G_{d2} v_d^2 \\ &\quad + G_{m3} v_g^3 + G_{m2d1} v_g^2 v_d + G_{m1d2} v_g v_d^2 + G_{d3} v_d^3. \end{aligned} \tag{8}$$

The time variable dependence has been dropped to shorten the notation. This small-signal drain current includes both the output conductance derivative terms (G_{d2} and G_{d3}) and the cross-derivative terms (G_{m1d1}, G_{m2d1}, and G_{m1d2}) which have been ignored in most of the nonlinear analyses. We have implemented this complete model in our analysis program. A study has been carried out to theoretically examine the importance of this complete model compared with the conventional model (only G_m, G_{m2}, and G_{m3} included) to the overall IMD performance of FET mixers. This is presented in the next section.

Due to the pump of the LO signal, all the coefficients in the Taylor's expansion are also time-varying functions. We expand the small-signal incremental voltages and limit consideration up to third order

$$v_p(t) = v_{p1}(t) + v_{p2}(t) + v_{p3}(t) \tag{9}$$

and

$$v_p^2(t) = v_{p1}^2(t) + 2v_{p1}(t)v_{p2}(t) \tag{10}$$

$$v_p^3(t) = v_{p1}^3(t) \tag{11}$$

where v_p represents v_g, v_f, and v_d.

In order to analyze the circuit in the frequency domain, the time-varying functions due to the LO pump have to be Fourier expanded into the harmonic components of the LO frequency ω_p. They have the form

$$G_x(t) = \sum_{h=-K}^{K} G_{x,h} e^{jh\omega_p t}. \tag{12}$$

In FET gate mixers, the RF signal is from the gate side, so $v_{sd} = 0$. The subscript g in the small-signal voltage source representing the source at the gate will be dropped. The small-signal voltage with Q input signals is

$$v_s(t) = \sum_{q=1}^{Q} 2V_{s,q} \cos(\omega_q t) = \sum_{\substack{q=-Q \\ q\neq 0}}^{Q} V_{s,q} e^{j\omega_q t} \tag{13}$$

where $2V_{s,q}$ is the voltage peak value of the qth input signal with frequency ω_q. Note that ω_{-q} is equal to $-\omega_q$.

The Taylor's expansion of the small-signal drain current is substituted in (1), and all the time-varying functions are expanded in frequency domain. The circuit equations can then be separated into subcircuits for different orders. They have the form

$$[\boldsymbol{ZY} - \mathbf{1}]\boldsymbol{V_n} = \boldsymbol{V_{sn}} \tag{14}$$

where

$$\boldsymbol{Y} = \begin{pmatrix} j\Omega \boldsymbol{C_{gs}} & 0 & 0 \\ 0 & 0 & j\Omega \boldsymbol{C_{gd}} \\ \boldsymbol{G_m} & 0 & \boldsymbol{G_{ds}} + j\Omega \boldsymbol{C_{ds}} \end{pmatrix}. \tag{15}$$

$\boldsymbol{G_m}$ and $\boldsymbol{G_{ds}}$ have the form of the conversion matrix in the conventional small-signal analysis of mixers. Note that the frequency matrix Ω has to reflect the frequencies of different orders. The impedances in impedance matrix $\boldsymbol{Z}$ also have to be evaluated at the corresponding frequencies of different orders. A short description of the subcircuits for different orders follows.

First order ($n = 1$):

$$\boldsymbol{V_1} = \begin{pmatrix} v_{g1} \\ v_{f1} \\ v_{d1} \end{pmatrix} \tag{16}$$

$$\boldsymbol{V_{s1}} = \begin{pmatrix} v_s \\ v_s \\ 0 \end{pmatrix}. \tag{17}$$

The first-order voltages in the frequency domain have the form

$$v_{p1}(t) = \sum_{m=-K}^{K} \sum_{\substack{q=-Q \\ q\neq 0}}^{Q} V_{p1,m,q} e^{j(m\omega_p + \omega_q)t} \tag{18}$$

which can be solved from the first-order circuit equations. The equivalent circuit for the first-order equations is shown in Fig. 4(a). After the first-order voltages are determined, the conversion gain/loss can be calculated between any two frequencies.

Second order ($n = 2$):

$$\boldsymbol{V_2} = \begin{pmatrix} v_{g2} \\ v_{f2} \\ v_{d2} \end{pmatrix} \tag{19}$$

$$\boldsymbol{V_{s2}} = -\boldsymbol{Z I_{s2}} \tag{20}$$

where

$$\boldsymbol{I_{s2}} = \begin{pmatrix} 0 \\ 0 \\ G_{m2} v_{g1}^2 + G_{d2} v_{d1}^2 + G_{m1d1} v_{g1} v_{d1} \end{pmatrix}. \tag{21}$$

Note that each element in matrices is a function of time. Since the first-order voltages have been solved, the second-order

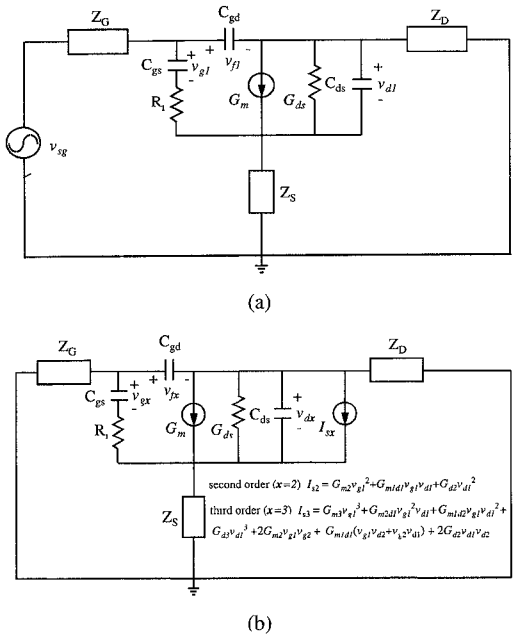

Fig. 4. (a) First-order small-signal equivalent circuit. (b) Second-order ($x = 2$) and third-order ($x = 3$) small-signal equivalent circuit.

nonlinear current source $\boldsymbol{I_{s2}}$ can be determined, where

$$G_{m2}(t)v_{g1}^2(t) = \sum_{h=-K}^{K}\sum_{m=-K}^{K}\sum_{n=-K}^{K}\sum_{\substack{q1=-Q\\ q1\neq 0}}^{Q}\sum_{\substack{q2=-Q\\ q2\neq 0}}^{Q} \cdot G_{m2,\,h}V_{g1,\,m,\,q1}V_{g1,\,n,\,q2} \cdot \exp\left(j[(h+m+n)\omega_p + \omega_{q1} + \omega_{q2}]t\right). \tag{22}$$

$G_{d2}v_{d1}^2$ and $G_{m1d1}v_{g1}v_{d1}$ have similar forms. The second-order voltages can be written as

$$v_{p2}(t) = \sum_{m=-K}^{K}\sum_{\substack{q1=-Q\\ q1\neq 0}}^{Q}\sum_{\substack{q2=-Q\\ q2\neq 0}}^{Q} V_{p2,\,m,\,q1,\,q2} \cdot \exp\left(j(m\omega_p + \omega_{q1} + \omega_{q2})t\right) \tag{23}$$

which can be solved from the second-order circuit equations. The equivalent circuit for the second-order equation is shown in Fig. 4(b) (with $x = 2$). Once the second-order voltages are known, the output power for any second-order distortion can be determined.

Third order ($n = 3$):

$$\boldsymbol{V_3} = \begin{pmatrix} v_{g3} \\ v_{f3} \\ v_{d3} \end{pmatrix} \tag{24}$$

$$\boldsymbol{V_{s3}} = -\boldsymbol{Z}\boldsymbol{I_{s3}} \tag{25}$$

where

$$\boldsymbol{I_{s3}} = \begin{pmatrix} 0 \\ 0 \\ a+b \end{pmatrix} \tag{26}$$

with

$$a = 2G_{m2}v_{g1}v_{g2} + G_{m3}v_{g1}^3 + 2G_{d2}v_{d1}v_{d2} + G_{d3}v_{d1}^3 \tag{27}$$

$$b = G_{m1d1}(v_{g1}v_{d2} + v_{g2}v_{d1}) + G_{m2d1}v_{g1}^2v_{d1} + G_{m1d2}v_{g1}v_{d1}^2 \tag{28}$$

in which

$$G_{m3}(t)v_{g1}^3(t) = \sum_{h=-K}^{K}\sum_{m=-K}^{K}\sum_{n=-K}^{K}\sum_{l=-K}^{K} \cdot \sum_{\substack{q1=-Q\\ q1\neq 0}}^{Q}\sum_{\substack{q2=-Q\\ q2\neq 0}}^{Q}\sum_{\substack{q3=-Q\\ q3\neq 0}}^{Q} G_{m3,\,h}V_{g1,\,m,\,q1} \cdot V_{g1,\,n,\,q2}V_{g1,\,l,\,q3}\exp\left(j[(h+m+n+l)\omega_p + \omega_{q1} + \omega_{q2} + \omega_{q3}]t\right) \tag{29}$$

$$G_{m2}(t)v_{g1}(t)v_{g2}(t) = \sum_{h=-K}^{K}\sum_{m=-K}^{K}\sum_{n=-K}^{K}\sum_{\substack{q1=-Q\\ q1\neq 0}}^{Q}\sum_{\substack{q2=-Q\\ q2\neq 0}}^{Q}\sum_{\substack{q3=-Q\\ q3\neq 0}}^{Q} G_{m2,\,h} \cdot V_{g1,\,m,\,q1}V_{g2,\,n,\,q2,\,q3}\exp\left(j[(h+m+n)\omega_p + \omega_{q1} + \omega_{q2} + \omega_{q3}]t\right) \tag{30}$$

and the other elements can be expanded into the frequency domain accordingly. The equivalent circuit for the third-order equations is shown in Fig. 4(b) (with $x = 3$).

The output power for any third-order IMD of interest can be determined from the third-order circuit equations. For instance, the frequency of the third-order IMD with two RF tones is either $|2f_{\mathrm{IF2}} - f_{\mathrm{IF1}} - f_p|$($q1 = 2$, $q2 = 2$, and $q3 = -1$) or $|2f_{\mathrm{IF1}} - f_{\mathrm{IF2}} - f_p|$($q1 = 1$, $q2 = 1$, and $q3 = -2$).

III. Nonlinear Sources in MESFET Gate Mixers

The most significant nonlinear element in a MESFET gate mixer is the drain current, which formally is a function of both gate (V_g) and drain voltage (V_d). The small-signal drain current expanded in Taylor's series up to third order has been given in (8).

Usually, the nonlinear transconductance (G_m, G_{m2}, and G_{m3}) is the only part of the nonlinear drain current which has been considered in the FET nonlinear applications. The influence from other terms in (8) on the overall nonlinear performance has been ignored. Recently, the authors of [8] proposed a technique to determine the values of G_m, G_{m2}, and G_{m3} from the measurement data at low frequency (50 MHz). The authors of [19] and [20] then extended the measurement technique, and proposed a new measurement setup which is able to extract the values of all the coefficients in (8). They included all of these coefficients in their load pull IM distortion simulation. They also demonstrated that the influence from

terms other than G_m, G_{m2}, and G_{m3} on the overall IM distortion of their load pull simulation is significant.

In order to determine the influence of all the terms in (8) on the overall IM distortion of FET gate mixers, we have carried out a simulation study using our analysis program. We have followed exactly the nonlinear characterization procedure at low frequency proposed in [19] and [20] to obtain all the coefficients in (8) for the device in our study. The sources we used for the low-frequency characterization were at 95 and 105 MHz. The device we used in this study is a MESFET fabricated in the Solid State Electronics Laboratory at the University of Michigan (the device will be denoted as SSEL in the rest of the text). This device has a gate geometry of 0.25 × 90 μm, a doping concentration of $5 \times 10^{17}\text{cm}^3$, a 600-Å-thick channel, and a pinch-off voltage of -2.0 V. We characterized this device at various gate and drain voltages. The gate voltage was varied from -3.0 to 0 V by steps of 0.1 V. The drain voltage was varied from 1.5 to 3.3 V by steps of 0.2 V. The values of all the coefficients extracted from this low-frequency characterization were then numerically implemented in the analysis program discussed in Section II. Linear interpolation was used to determine the values between the measured data points. Single-tone IM of an X-band mixer with LO at 10.8 GHz and RF at 11.1 GHz was simulated for two different cases: one using all the coefficients, and the other only using the nonlinearity of the transconductance and its derivatives (G_m, G_{m2}, and G_{m3}). Simple 50-Ω source and 50-Ω load impedances were used in this study. A dc drain voltage of 2.5 V was chosen as a bias point to compare the theoretical results of this two cases. The signals at two times and three times the frequency of the IF signal, i.e., 600 and 900 MHz, were the single-tone IM products at the output. In Fig. 5, we show the simulation results of these two cases for a 4.63 dBm LO power. The results show no significant difference between these two cases, which means the contributions from terms other than G_m, G_{m2}, and G_{m3} to the overall IMD of the FET gate mixers are much smaller than those of the dominant terms, G_m, G_{m2}, and G_{m3}. They, in effect, can be ignored.

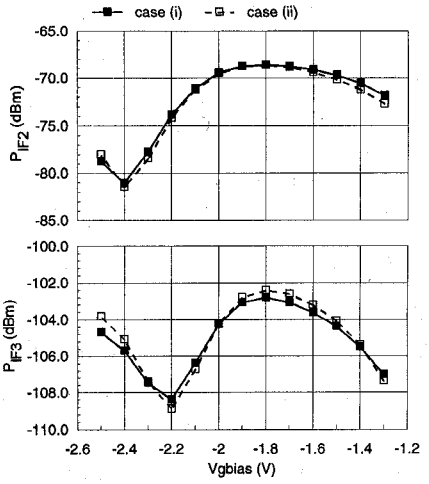

Fig. 5. Comparison of single-tone IM simulation of the SSEL MESFET gate mixer between two cases: case (i) with the full nonlinear drain current model in (8) and case (ii) with only G_m, G_{m2}, and G_{m3} included. The mixer has a simple 50-Ω source and a 50-Ω load impedance. 2.5 V of the drain voltage is chosen. $f_{\text{LO}} = 10.8$ GHz, $f_{\text{RF}} = 11.1$ GHz, $f_{\text{IF2}} = 600$ MHz, and $f_{\text{IF3}} = 900$ MHz. $P_{\text{LO}} = 4.63$ dBm, and $P_{\text{RF}} = -20.66$ dBm.

IV. The Proposed Nonlinear Model

The essential issue of modeling the nonlinear drain current centers on how accurately the coefficients G_m, G_{m2}, and G_{m3} can be described. A common approach is to model the drain current function itself [8], [10]–[14]. The drawback of this approach is that any error occurring in the drain current function will propagate down to all its derivatives. Most of the existing drain current models [10]–[13] did not take derivatives into consideration when they originally were proposed. Consequently, these models have an inadequate description of G_{m2} and G_{m3}, the second and third derivatives of the drain current function with respect to the gate voltage. Therefore, these models basically are not suitable for IM analysis. In order to avoid this shortcoming, we propose a direct model of the second derivative of the drain current with respect to gate voltage (G_{m2}) instead of the drain current function, which greatly simplifies the fitting process of the model. The proposed functional dependence of the second derivative is a Gaussian function plus a linear modification term. The functions for G_m and G_{m3} are easily derived from G_{m2} by simple integration and differentiation with respect to the gate voltage. The proposed functions for G_m, G_{m2}, and G_{m3} are as follows:

$$G_m = G'_{mx} v_{g\sigma} \sqrt{\pi} \left(1 + \text{erf}\left(\frac{v_g - v_{gp}}{v_{g\sigma}}\right)\right) + G''_{m0}(v_g - v_{g\gamma})^2 \tag{31}$$

$$G_{m2} = G'_{mx} e^{-((v_g - v_{gp})/v_{g\sigma})^2} + G''_{m0}(v_g - v_{g\gamma}) \tag{32}$$

$$G_{m3} = -\frac{2}{3}\frac{G'_{mx}}{v_{g\sigma}^2}(v_g - v_{gp}) e^{-((v_g - v_{gp})/v_{g\sigma})^2} + \frac{1}{3} G''_{m0}. \tag{33}$$

G'_{mx}, G''_{m0}, v_{gp}, $v_{g\sigma}$, and $v_{g\gamma}$ are the fitting parameters. G'_{mx}, v_{gp}, and $v_{g\sigma}$, which are the peak value, the location of the peak value, and the half-width of the Gaussian function, respectively, can be approximately determined just from the plot of data for G_{m2}. This simplifies the fitting between the model and the measurement data. All the parameters can be easily determined from a simple least-square fit to data determined from low-frequency measurements. The fitting results of G_m, G_{m2}, and G_{m3} for the SSEL MESFET at $V_D = 2.5$ V are shown in Fig. 6. The agreement between the model and the measurement data is considered excellent.

All of these fitting parameters are, strictly speaking, functions of drain voltage, but since, in the case of the gate mixer, the device is biased in the saturation region, the variation due to the drain voltage can be ignored.

Although this simplified model was originally constructed for the MESFET mixers, it can be used for HEMT mixers as well. Even though HEMT's have quite different characteristics of transconductance versus gate voltage compared to MESFET's this model also can fit G_m, G_{m2}, and G_{m3} very well due to the extra linear function of gate voltage used in G_{m2}. The same low-frequency nonlinear characterization

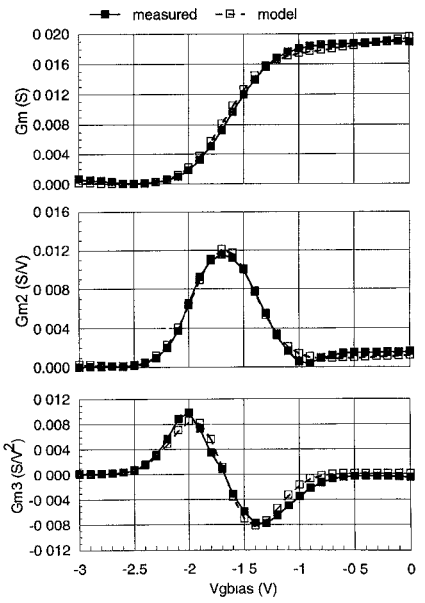

Fig. 6. Comparison of G_m, G_{m2}, and G_{m3} between the measurement and the proposed model for the SSEL MESFET at $V_D = 2.5$ V. The fitting parameters are: $G'_{mx} = 0.01174$, $G''_{m0} = 4.9 \times 10^4$, $v_{gp} = -1.68$, $v_{g\sigma} = 0.40$, and $v_{g\gamma} = -2.45$.

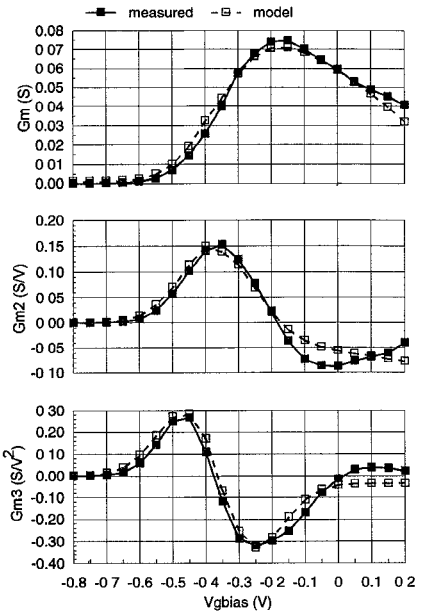

Fig. 7. Comparison of G_m, G_{m2}, and G_{m3} between the measurement and the proposed model for the NE324 HEMT at $V_D = 2.0$ V. The fitting parameters are: $G'_{mx} = 0.160$, $G''_{m0} = -0.105$, $v_{gp} = -1.358$, $v_{g\sigma} = 0.157$, and $v_{g\gamma} = -0.530$.

procedure for MESFET was also applied to HEMT in order to obtain the values of G_m, G_{m2}, and G_{m3} experimentally. The HEMT device used in this study is a commercial product from NEC, model NE324. In Fig. 7, the fitting result of the model is compared with the measurement data at $V_D = 2.0$ V for G_m, G_{m2}, and G_{m3}. In order to achieve better fit, the linear term in G_{m2} is only included for the gate voltage greater than v_{gp}. Good agreement between measurement and the proposed model is observed, which shows the ability of this model to fit the nonlinear transconductance of HEMT's.

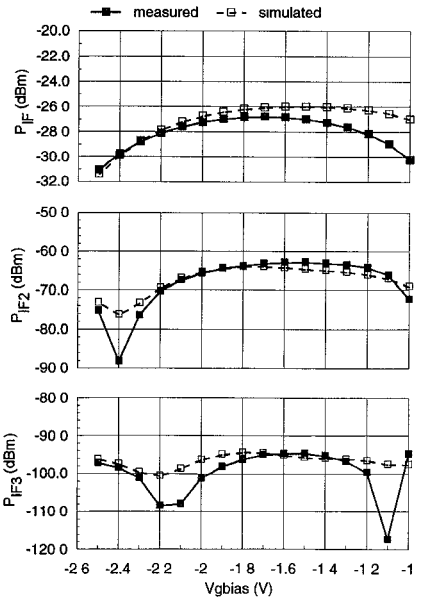

Fig. 8. Measured and calculated single-tone IM results of the SSEL MESFET gate mixer for $V_D = 2.5$ V with a simple 50-Ω source and a 50-Ω load impedance. $f_{\rm LO} = 10.8$ GHz, $f_{\rm RF} = 11.1$ GHz, $f_{\rm IF} = 300$ MHz, $f_{\rm IF2} = 600$ MHz, and $f_{\rm IF3} = 900$ MHz. $P_{\rm LO}$ =4.63 dBm and $P_{\rm RF} = -20.66$ dBm.

V. X-Band Mixer Results

To verify the adequacy of the model for the IMD analysis of MESFET mixers, we made single-tone IM measurements on two different MESFET mixers, one using the SSEL MESFET, and the other a commercial MESFET (model NE71000 from NEC). The devices were bonded on chip carriers and measured in an X-band test fixture. The sole purpose of this measurement was to verify the validity of the proposed model. So, no matching was attempted for either input or output circuits. Both mixer circuits had a simple 50-Ω source and a 50-Ω load impedance. The LO and RF at 10.8 and 11.1 GHz, respectively, were applied to the gate and IF output at 300, 600, and 900 MHz were measured at the drain. The measured and calculated results for the SSEL MESFET mixer and the NE71000 MESFET mixer are shown in Figs. 8 and 9, respectively. In Fig. 10, we show the measured and calculated second-order and third-order output power versus RF input power for the SSEL MESFET mixer under the same bias and LO power condition as in Fig. 8. The calculated second-order and third-order intercept points ($IP2$ and $IP3$, respectively) are also marked in the figure. All of the simulation results are obtained from the analysis program discussed in Section II. 12 harmonics of the LO frequency were chosen for all the simulations. Even though 12 harmonics were used, the simulation program required only about 1 min. of computation time for each point on a Sun/SPARC 10 workstation. Good agreement between the measured and calculated results was obtained for both mixers.

We then applied our simplified model to a two-tone IMD simulation. The two-tone IM measurement was performed on the NE71000 MESFET mixer. An additional RF source at 11.2 GHz was added to the gate of the previous setup, and the third-order IM product, $2f_{\rm IF2} - f_{\rm IF1} - f_p$, at 500 MHz was measured at the output. The results of this measurement along with the

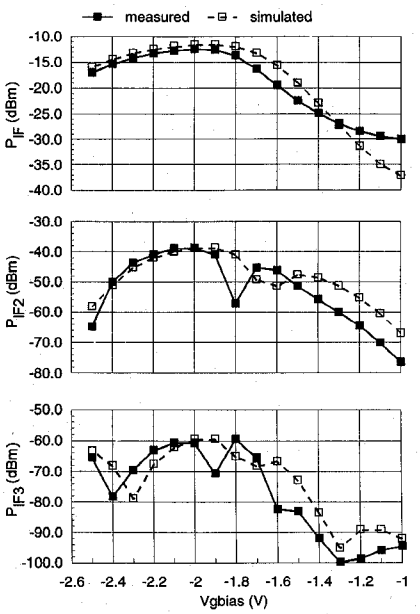

Fig. 9. Measured and calculated single-tone IM results of the NE71000 MESFET gate mixer for $V_D = 2.7$ V with a simple 50-Ω source and a 50-Ω load impedance. $f_{\rm LO} = 10.8$ GHz, $f_{\rm RF} = 11.1$ GHz, $f_{\rm IF} = 300$ MHz, $f_{\rm IF2} = 600$ MHz, and $f_{\rm IF3} = 900$ MHz. $P_{\rm LO} = 3.0$ dBm and $P_{\rm RF} = -10.22$ dBm.

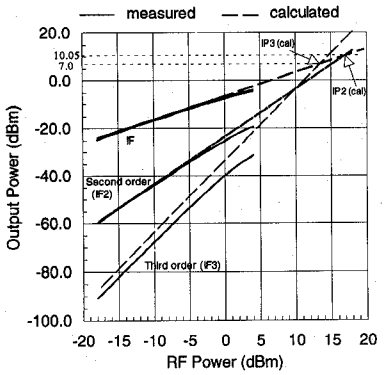

Fig. 10. Calculated single-tone $IP2$ and $IP3$ of the SSEL MESFET along with the measured data. Gate bias of -1.8 V is chosen. Check Fig. 8 for the values of drain bias, LO power, and signal frequencies.

calculated results from the analysis program are shown in Fig. 11. The good agreement shown again supports the validity of the simplified model for the IM analysis of MESFET gate mixers and the accuracy of the analysis program for multitone IMD simulation.

We also made single-tone and two-tone IM measurements of a HEMT mixer at X band. The device used in the mixer measurement is the same device mentioned in Section IV. The device was bonded on the same type of chip carrier used for the MESFET's. The same measurement setup was also used.

The comparison of the calculated IF power, second- and third-order IM products for the single-tone case with the measurement results is shown in Fig. 12. The comparison for the third-order IM product for the two-tone case is shown in Fig. 13. The good agreement conforms the validity of the proposed simplified model applied to HEMT mixers.

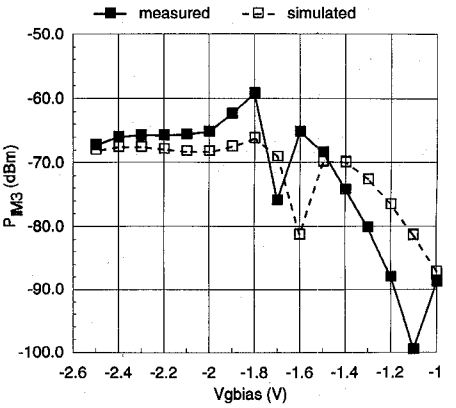

Fig. 11. Measured and calculated two-tone IM results of the NE71000 MESFET gate mixer for $V_D = 2.7$ V with a simple 50-Ω source and a 50-Ω load impedance. $f_{\rm LO} = 10.8$ GHz, $f_{\rm RF1} = 11.1$ GHz, $f_{\rm RF2} = 11.2$ GHz, and $f_{\rm IM3} = 500$ MHz. $P_{\rm LO} = 3.0$ dBm, $P_{\rm RF1} = -17.0$ dBm, and $P_{\rm RF2} = -11.0$ dBm.

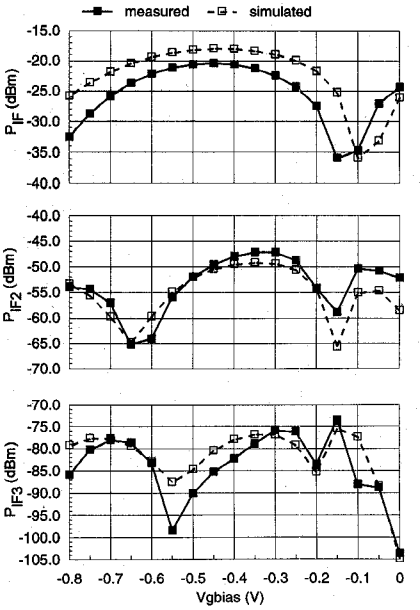

Fig. 12. Measured and calculated single-tone IM results of the NE324 HEMT gate mixer for $V_D = 2.0$ V with a simple 50-Ω source and a 50-Ω load impedance. $f_{\rm LO} = 10.8$ GHz, $f_{\rm RF} = 11.1$ GHz, $f_{\rm IF} = 300$ MHz, $f_{\rm IF2} = 600$ MHz, and $f_{\rm IF3} = 900$ MHz. $P_{\rm LO} = -2.0$ dBm and $P_{\rm RF} = -21.67$ dBm.

VI. Conclusion

An efficient and accurate analysis program has been developed for the IM simulation of FET mixers. The technique used in this program is based on the *large-signal–small-signal analysis*. This program can avoid the common problem encountered in the commercial microwave circuit simulators (e.g., LIBRA) for the IM analysis of mixers. Since these simulators use the general-purpose harmonic balance technique to analyze the LO and RF signals simultaneously, the third-order IM distortion from the much smaller RF signals, compared to the LO signal, will be smeared out by the large LO signal through the discrete Fourier transform due to the roundoff error of the computer. Even though multitone excitations are available in these simulators, the computer running time will

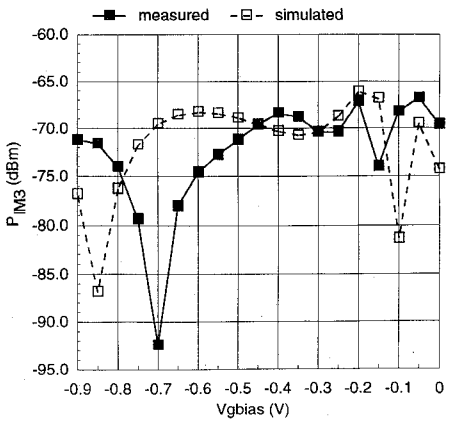

Fig. 13. Measured and calculated two-tone IM results for the NE324 HEMT gate mixer for $V_D = 2.0$ V with a simple 50-Ω source and a 50-Ω load impedance. $f_{LO} = 10.8$ GHz, $f_{RF1} = 11.1$ GHz, $f_{RF2} = 11.2$ GHz, and $f_{IM3} = 500$ MHz. $P_{LO} = -2.0$ dBm, $P_{RF1} = -21.67$ dBm, and $P_{RF2} = -22.70$ dBm.

be dramatically increased with the number of excitations. This makes the IM analysis of mixers almost impractical using these simulators.

A detailed study was carried out to examine the influence on the IM distortion of the MESFET gate mixers from the nonlinear factors in the drain current other than the nonlinearity of the transconductance with respect to gate voltage. The study shows that the influence is small, and the nonlinear transconductance alone is adequate to describe the IM distortion in the FET gate mixers. Then, a simplified nonlinear model for the transconductance was proposed. This model uses the sum of a Gaussian function and a linear function of gate voltage for the derivative of the transconductance (G_{m2}). The fitting parameters of the model can be easily determined by an intuitive examination from the low-frequency characterization of the transconductance nonlinearity and a simple least square fit. The calculated results from this model are in good agreement with experimental data. The accuracy of the model for the IM analysis of FET mixers has been verified experimentally by two different MESFET mixers and one HEMT mixer at X band. The good agreement between the measurement and simulation shows the validity of the model for both MESFET and HEMT mixers.

ACKNOWLEDGMENT

The authors thank K. Moore for fabricating the SSEL MESFET's and C.-Y. Chi for device bonding.

REFERENCES

[1] A. Ushida and L. Chua, "Frequency-domain analysis of nonlinear circuits driven by multitone signals," *IEEE Trans. Circuits Syst.*, vol. CAS-31, pp. 766–778, Sept. 1984.
[2] R. Gilmore, "Nonlinear circuit design using the modified harmonic balance algorithm," *IEEE Trans. Microwave Theory Tech.*, vol. MTT-34, pp. 1294–1307, Dec. 1986.
[3] W. R. Curtice, "Nonlinear analysis of GaAs MESFET amplifiers, mixers, and distributed amplifiers using the harmonic balance technique," *IEEE Trans. Microwave Theory Tech.*, vol. MTT-35, pp. 441–447, May 1987.
[4] C. C. Pénalosa and C. S. Aitchison, "Analysis and design of MESFET gate mixers," *IEEE Trans. Microwave Theory Tech.*, vol. MTT-35, pp. 643–652, July 1987.
[5] J. J. Bussgang, L. Ehrman, and J. W. Graham, "Analysis of nonlinear systems with multiple inputs," *Proc. IEEE*, vol. 62, pp. 1088–1119, Aug. 1974.
[6] R. A. Minasian, "Volterra series analysis of MESFET mixers," *Int. J. Electron.*, vol. 50, no. 3, pp. 215–219, 1981.
[7] S. A. Maas, "Two-tone intermodulation in diode mixers," *IEEE Trans. Microwave Theory Tech.*, vol. MTT-35, pp. 307–314, Mar. 1987.
[8] S. A. Maas and D. Neilson, "Modeling MESFET's for intermodulation analysis of mixers and amplifiers," *IEEE Trans. Microwave Theory Tech.*, vol. 38, pp. 1964–1971, Dec. 1990.
[9] S. A. Maas, "How to model intermodulation distortion," in *IEEE MTT Symp. Dig.*, 1991, pp. 149–151.
[10] W. R. Curtice, "A MESFET model for use in the design of GaAs integrated circuits," *IEEE Trans. Microwave Theory Tech.*, vol. MTT-28, pp. 448–456, May 1980.
[11] W. R. Curtice and M. Ettenberg, "A nonlinear GaAs FET model for use in the design of output circuits for power amplifiers," *IEEE Trans. Microwave Theory Tech.*, vol. MTT-33, pp. 1383–1394, Dec. 1985.
[12] A. Materka and T. Kacprzak, "Computer calculation of large-signal GaAs FET amplifier characteristics," *IEEE Trans. Microwave Theory Tech.*, vol. MTT-33, pp. 129–135, Feb. 1985.
[13] H. Statz, P. Newman, I. Smith, R. Pucel, and H. Haus, "GaAs FET device and circuit simulation in SPICE," *IEEE Trans. Electron Dev.*, vol. ED-34, pp. 160–169, Feb. 1987.
[14] I. Angelov, H. Zirath, and N. Rorsman, "A new empirical nonlinear model for HEMT and MESFET devices," *IEEE Trans. Microwave Theory Tech.*, vol. 40, pp. 2258–2266, Dec. 1992.
[15] S. A. Maas, *Nonlinear Microwave Circuits*. Norwood, MA: Artech House, 1988.
[16] A. R. Kerr, "A technique for determining the local oscillator waveforms in a microwave mixer," *IEEE Trans. Microwave Theory Tech.*, vol. MTT-23, pp. 828–831, Oct. 1975.
[17] P. H. Siegel and A. R. Kerr, "A user oriented computer program for the analysis of microwave mixers, and a study of the effects of the series inductance and diode capacitance on the performance on the performance of some simple mixers," NASA Tech. Memo. 80324, NASA Goodard Space Flight Center, Greenbelt, MD, July 1979.
[18] S. A. Maas, *Microwave Mixers*, 1st ed. Norwood, MA: Artech House, 1985.
[19] J. C. Pedro and J. Perez, "An improved MESFET model for prediction of intermodulation load-pull characterization," in *IEEE MTT-S Dig.*, 1992, pp. 825–828.
[20] ——, "Accurate simulation of GaAs MESFET's intermodulation distortion using a new drain-source current model," *IEEE Trans. Microwave Theory Tech.*, vol. 42, pp. 25–33, Jan. 1994.

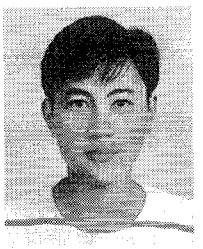

Solti Peng (S'90) was born in Kaohsung, Taiwan, on February 3, 1964. He received the B.S. degree in physics from the National Cheng-Kung University, Taiwan, in 1984, and the M.S. degree in electrical engineering from the University of Michigan, Ann Arbor, in 1990.

Since then, he has been working toward the Ph.D. degree in the Department of Electrical Engineering at the University of Michigan.

Patrick J. McCleer (S'67–M'69–S'71–M'71–S'75–S'78–M'78) received the B.S. degree from the University of Michigan, Ann Arbor, in 1969, the M.S. degree from M.I.T., Cambridge, in 1972, and the Ph.D. degree, also from the University of Michigan, in 1978, all in electrical engineering.

He is President of McCleer Power, Inc., a small firm in Jackson, MI, which specializes in research and development, and prototype fabrication of power electronic system and electrical machines. He is also a part time associate research scientist in the Department of Electrical Engineering, University of Michigan.

Dr. McCleer is a Registered Professional Engineer in the State of Michigan.

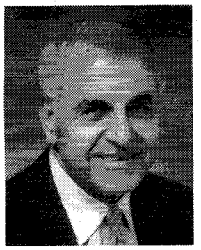

George I. Haddad (S'57–M'61–SM'66–F'72) received the B.S.E., M.S.E., and Ph.D. degrees in electrical engineering from the University of Michigan, Ann Arbor.

From 1957–1958 he was associated with the Engineering Research Institute of the University of Michigan, where he was engaged in research on electromagnetic accelerators. In 1958 he joined the Electron Physics Laboratory, where he was engaged in research on masers, parametric amplifiers, detectors, and electron-beam devices. From 1960–1969 he served successively as instructor, assistant professor, associate professor, and professor in the Electrical Engineering Department. He served as Director of the Electron Physics Laboratory from 1968–1975. From 1975–1987 he served as Chairman of the Department of Electrical Engineering and Computer Science. From 1987–1990 he was Director of both the Solid-State Electronics Laboratory and the Center for High-Frequency Microelectronics. He is currently the Robert J. Hiller Professor and Chairman of the Electrical Engineering and Computer Science Department and Director of the Center for High Frequency Microelectronics. His current research areas are microwave and millimeter-wave solid-state devices and monolithic integrated circuits, microwave-optical interactions, and optoelectronic devices and integrated circuits.

Dr. Haddad received the 1970 Curtis W. McGraw Research Award of the American Society for Engineering Education for outstanding achievements by an engineering teacher, the College of Engineering Excellence in Research Award (1985), the Distinguished Faculty Achievement Award (1986) of the University of Michigan, and the S. S. Attwood Award of the College of Engineering for Outstanding Contributions to Engineering Education, Research, and Administration. He is a member of Eta Kappa Nu, Sigma Xi, Phi Kappa Phi, Tau Beta Pi, and American Society for Engineering Education, and the American Physical Society. He is a member of the National Academy of Engineering.